

RELAXOR FERROELECTRICS: USEFUL ELECTRONIC NANOCOMPOSITE STRUCTURES

L. ERIC CROSS

Materials Research Laboratory, The Pennsylvania State University, University Park, PA
16802-4800 USA.

Abstract The paper will discuss the current status of understanding of the ferroelectric relaxors which are a sub group of the larger family of ferroelectrics with diffuse phase transitions. In the lead magnesium niobate (PMN) and lead scandium tantalate (PST) systems limited B site cation ordering appears to break the long range translational symmetry giving rise to the glass like behavior associated with the freeze out of polar fluctuations. In PMN and PST of major interest is the extent to which the spin glass models can describe the full range of elasto dielectric properties.

In the lead lanthanum zirconate titanate (PLZT) family the symmetry breaking phenomenon is not so clear and new work on the break up of conventional ferroelectricity in the lead lanthanum titanate (PLT) system will be discussed. A wide range of tungsten bronze family materials also exhibit relaxor ferroelectric behavior with unusual freezing behavior and switching capability.

In practical application the use of relaxor compositions in capacitor and electrostrictive actuator systems will be highlighted. New used in surface deformable mirrors and in a tilt mirror corrector for the Hubble Space Telescope will be presented.

INTRODUCTION

It is perhaps useful to begin the discussion of the interesting sub group of relaxor ferroelectrics by considering in a more general way the nature of the Curie point transition which heralds the onset of proper ferroelectric behavior. In figure 1a is illustrated first the behavior in a rather perfect single crystal which goes through an abrupt second order phase transition into the ferroelectric phase. Above T_c , the permittivity follows a Curie Weiss law $\epsilon^1 = C(T - T_c)^{-1}$, at T_c there is an abrupt but continuous onset of spontaneous polarization which evolves into the domain structure of the ferroelectric form. In some crystals the transition at T_c is first order, there is a finite maximum of ϵ at T_c and the Curie Weiss temperature θ in the relation $\epsilon = C(T - \theta)^{-1}$ occurs some degrees below T_c e.g. 11°C in BaTiO_3 . Again there is an abrupt loss of polarization at T_c now in a discontinuous step but ϵ_{max} and $P_s \rightarrow 0$ occur at the same temperature T_c .

For many practical applications it is desired to use the very large property maxima in the vicinity of the ferroelectric phase transition, to move the transition into the temperature range of interest and to broaden and diffuse the very large sharp peak values. In solid solution systems this is accomplished by trimming the mean composition to move the Curie point and at the same time

making the sample (often a ceramic) deliberately inhomogeneous. In these diffuse transition systems the dielectric maximum is now much 'rounder' and polarization persists for a short range of temperature above T_m (figure 1b). Almost all practical Z5U and Y5V capacitor dielectrics use such diffuse transitions.

In the relaxor ferroelectrics, three features of the dielectric response are qualitatively different. The transition is clearly diffuse and rounded, but the response is now markedly dispersive below T_m and T_m is a function of frequency (figure 1c). The response at weak fields above T_m is no longer Curie Weiss. In the polarization the RMS value persists to temperature (T_D) 200 to 300°C above T_m but the mean polarization \bar{P} decays to zero at a temperature T_F which is well below T_m .

The weak field dielectric behavior for a typical relaxor ferroelectric in the perovskite structure family, lead magnesium niobate, is shown in more detail in figure 2a, taken from the pioneer work of Smolensky,¹ the dispersion over the frequency range 10 Hz to 10^7 Hz is clearly evident. That the material is ferroelectric is evident from figure 2b which traces the evolution of dielectric hysteresis under high field as a function of temperature. Unlike the sharp transition materials there are not abrupt changes and non linearity persists to temperature well above T_m . Perhaps the most puzzling feature is the absence of evidence for any macroscopic phase change below T_m either in the X-rays spectra, or the optical birefringence (figure 2c), yet clearly spontaneous polarization is impossible in cubic symmetry.

The original explanation offered by Bokov and Mylnikova² for this behavior was that the diffuseness was again due to heterogeneity, giving a range of Curie points, but that now the scale was very small and therefore below the resolution of X-ray and optical probes (figure 3a). Considering this model of nano-scale polar regions, it appeared probable to us that since the energy barriers to reorientation in any ferroelectric are linearly related to the volume, at these very fine scales the electrocrystalline anisotropy energy ΔH_r might become comparable to kT leading to super-paraelectric behavior at higher temperature.

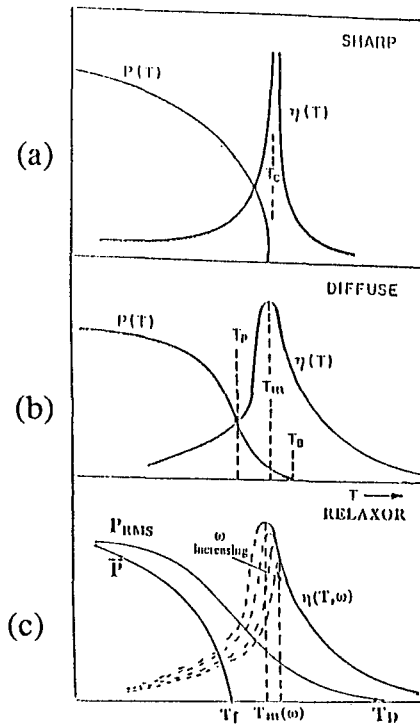


FIGURE 1 Types of Ferroelectric Phase Transitions

- (a) Simple proper ferroelectric: shape second order phase change in highly perfect single crystal.
- (b) Diffuse phase transition associated with macroscopic heterogeneity as in practical capacitor dielectrics.
- (c) Relaxor ferroelectric defining $T_m(\omega)$, T_D , T_F .

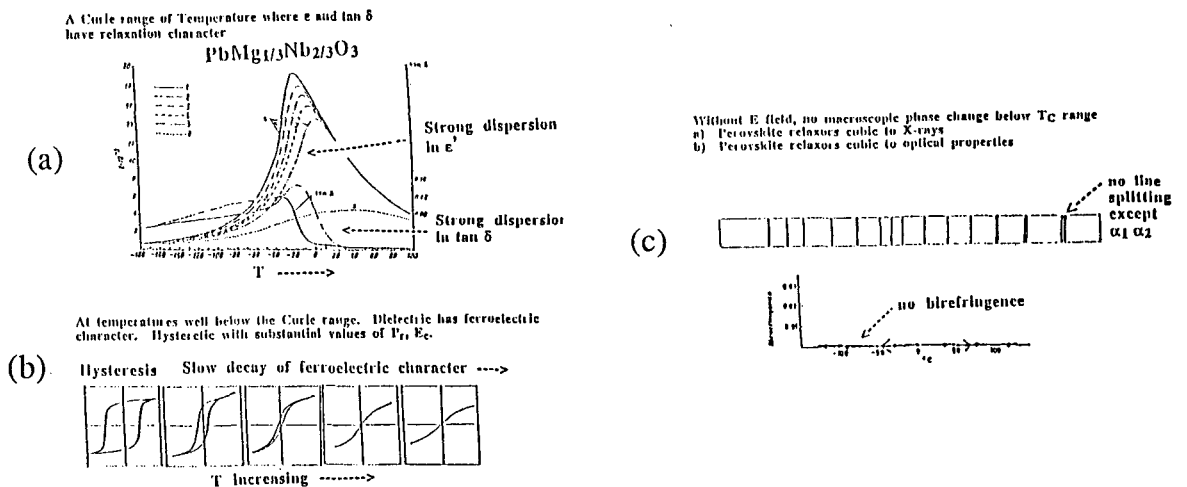


FIGURE 2 (a) Dispersion around T_m is Lead Magnesium niobate PMN, a typical relaxor ferroelectric.
 (b) Slow decay of polarization with temperature.
 (c) Absence of a macroscopic symmetry change.

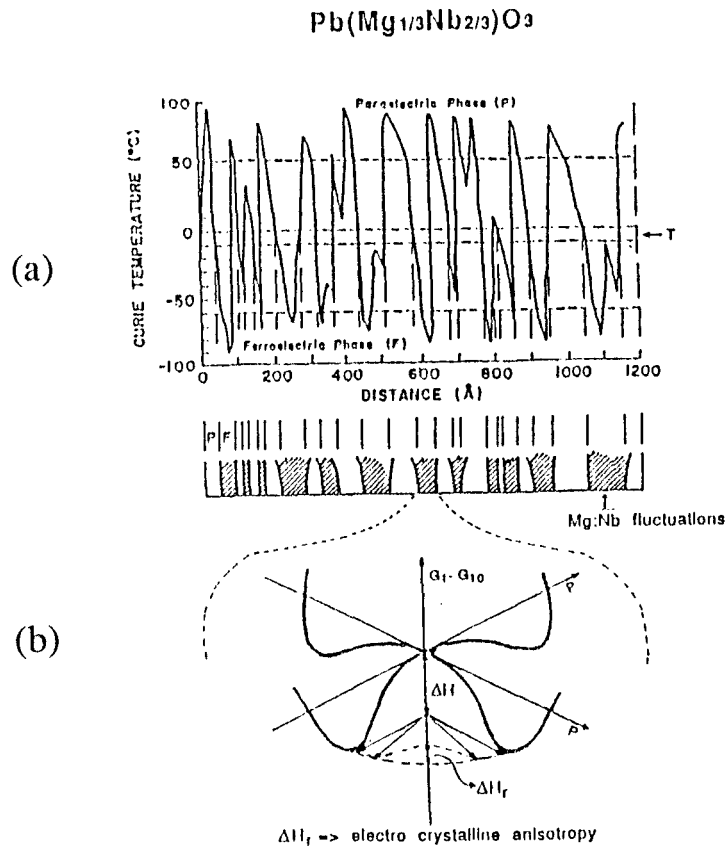


FIGURE 3 (a) Suggested compositional heterogeneity model after Smolensky.
 (b) Loss of stability with scale for very small micropolar regions.

A range of perovskite structure compounds with complex composition and a number of Tungsten bronze structure materials (Table I) show relaxor ferroelectric behavior. In perovskites the behavior occurs dominantly in lead based compositions and in both perovskites and bronzes there is always more than one type of ion occupying crystallographically equivalent sites.

For this brief review we will discuss first the origin of the symmetry breaking which occurs in the pre-cursors chemistry of these systems. It is reasonably well understood in $A(\text{B}_1\text{B}_2)\text{O}_3$ compositions but is less clear in the PLZTs and bronze family materials. Then the detail of the dielectric response which points towards a spin glass model for the freeze out of polar fluctuations as the origin of the dispersion will be considered. We then touch on some new evidence for unusual relaxor behavior in the low temperature polar phase of the tungsten bronze systems.

TABLE I. Systems Which Exhibit Relaxor Ferroelectric Behavior

PEROVSKITES OF COMPLEX COMPOSITIONS

B-site complex	Lead magnesium niobate (PMN)	$\text{PbMg}_{1/3}\text{Nb}_{2/3}\text{O}_3$
	Lead scandium tantalate (PST)	$\text{PbSc}_{1/2}\text{Ta}_{1/2}\text{O}_3$
	Lead zinc niobate (PZN)	$\text{PbZn}_{1/2}\text{Nb}_{1/2}\text{O}_3$
	Lead indium niobate (PIN)	$\text{PbIn}_{1/2}\text{Nb}_{1/2}\text{O}_3$
A-site	Lead lanthanum zirconate titanate (PLZT)	$\text{Pb}_{1-x}\text{La}_{2x/3}\text{TiO}_3$
	Lead lanthanum titanate (PLT)	$\text{Pb}_{1-x}\text{La}_{2x/3}\text{TiO}_3$
Both sites complex	Potassium lead zinc niobate	$\text{K}_{1/3}\text{Pb}_{2/3}\text{Zn}_{2/9}\text{Nb}_{7/9}\text{O}_3$

TUNGSTEN BRONZE STRUCTURE COMPOSITIONS

Sr _{1-x} Ba _x Nb ₂ O ₆	$\text{Sr}_{1-x}\text{Ba}_x\text{Nb}_2\text{O}_6$
Pb _{1-x} Ba _x Nb ₂ O ₆	$\text{Pb}_{1-x}\text{Ba}_x\text{Nb}_2\text{O}_6$

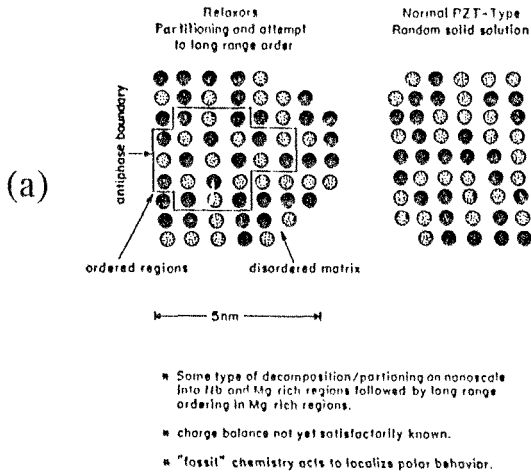
PERCURSON CHEMISTRY

In the lead based perovskite $\text{A}(\text{B}_1\text{B}_2)\text{O}_3$ relaxors it is clear from very extensive TEM studies^{3,4,5} that in $\text{Pb}(\text{Mg}_{1/3}\text{Nb}_{2/3})\text{O}_3$ the origin of the nanoscale heterogeneity is in a strictly limited 1:1 non stoichiometric ordering of the Mg and Nb. A crude two dimensional picture is given in figure 4a showing the scale of the region's which are of the order 5 n meters. The dark field TEM image confirming the ordering and the scale is shown in figure 4b.

This 1:1 ordering must give rise to a significant charge imbalance and it has been suggested⁶ that the developing electric field limits the scale. In $\text{PbSc}_{1/2}\text{Ta}_{1/2}\text{O}_3$ the ordering which is again 1:1 may be carried through to a highly ordered form by controlled thermal annealing, recovering full translational symmetry.⁷ It is important to note that the nano scale ordered PST exhibits relaxor behavior whilst the highly ordered crystal shows a first order ferroelectric phase change.

Our picture of relaxor behavior in the $\text{A}(\text{B}_1\text{B}_2)\text{O}_3$ systems is suggested schematically in figure 5. Either complete disorder, or full long range order appears to give rise to normal ferroelectric behavior. It is the limited nano-scale ordering which appears to favor the development of small scale polar regions. The fascinating feature in the PMN type compounds is that the non stoichiometry inherent in the ordering process appears to make it a self limiting nano-composite which cannot be changed by

NANOSCALE CHEMISTRY



(b)

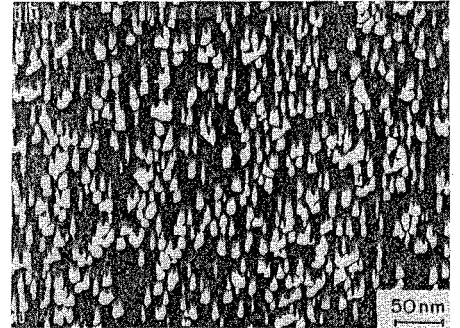


FIGURE 4 (a) Two dimensional sketch of observed 1:1 ordering of Mg:Nb cations in PMN.
(b) Dark field TEM and PMN showing the scale of the ordered regions.

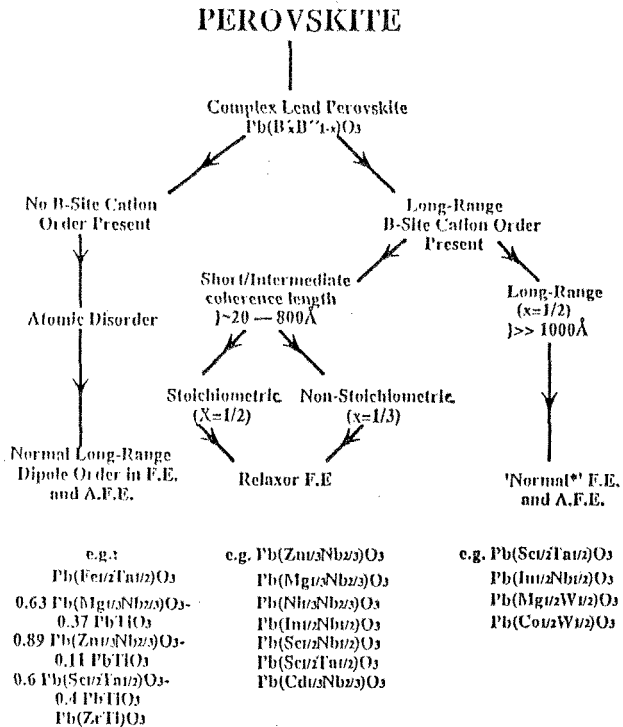
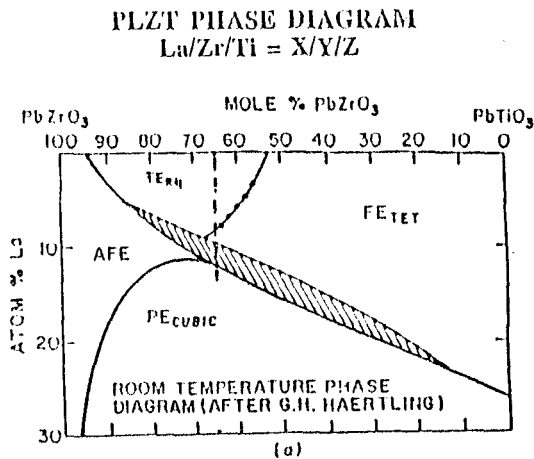


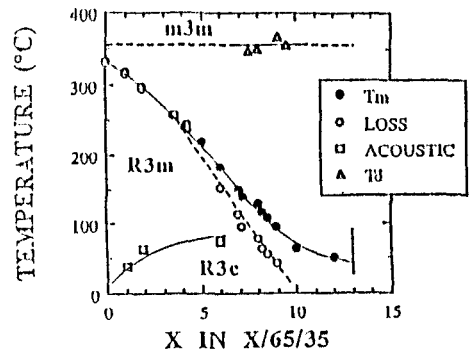
FIGURE 5 Suggested dependence of relaxor behavior in perovskite $Pb(B_1B_2)O_3$ compositions on limited $B_1:B_2$ ordering.

annealing. It should be emphasized that this is a most unusual nano-composite as the oxygen lattice is continuous and coherent through both ordered and disordered regions.

In the mixed A site relaxors such as the PLZTs with compositions along the 65:35 Zr:Ti mole ratio and Lanthanum concentration of more than 2 mole% (figure 6) the dielectric response is similar in many respects to the PMN system, however the symmetry breaking nanostructure is not so clear. Very careful TEM studies have revealed direct evidence of nano scale polar regions at low temperature⁸ but the precursor chemistry which forces their formation is not yet clear. Very recently Rossetti⁹ has explored the Lead lanthanum titanate system with high resolution X-ray techniques. It is clear that quite low levels of Lanthanum concentration rapidly reduce the strongly first order nature of the pure PbTiO_3 Curie point transition and begin to lead to a sub domain modulation of the magnitude of P_s in the domain, although there is no strong evidence for ordering of the lanthanum or the associated lead site vacancies at the higher concentrations. The necessary high defect concentration in the PLZT does however lead to an aging phenomenon¹⁰ which modifies the relaxation response markedly making longer time measurements of response impossible to interpret unequivocally.



(a)



(After Meltzler and O'Bryan)

(b)

FIGURE 6 (a) PLZT phase diagram showing the trace of the x:65:35 compositions studied.
(b) Evidence of the separation of T_m and T_d in these relaxor compositions.

In the tungsten bronze family, Barium strontium niobate $Ba_xSr_{1-x}Nb_2O_6$ is a prototypic relaxor here the structure is much more complex than the perovskite and more open. Again it is built on corner linked oxygen octahedra, but the sheet normal to the c axis of the tetragonal paraelectric form figure 7 is markedly crumpled. Here Nb ions occupy the centers of the oxygen octahedra, Ba ions the larger 5 fold channels and strontium are distributed between 4 fold and 5 fold channels. X-ray studies using the Rietveld method¹¹ suggest that Ba is always in the 5 fold channel but that annealing can change the Sr occupancy between 4 fold and 5 fold sites. Changing Sr occupancy has a marked effect upon the dielectric peak position T_m and it is suggested that variations in distribution throughout the crystal may be responsible for a wide distribution of local Curie points. It is interesting to note that the relaxation phenomenon becomes steadily stronger with increasing Sr concentration.

Much more work is however needed to pin down the symmetry breaking nonstructures in both the PLZTs and the bronze compositions.

Ferroelectric Tungsten Bronze Crystallographic Structure

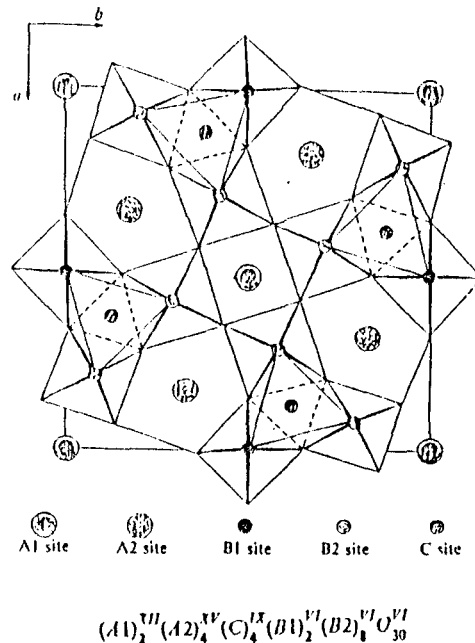
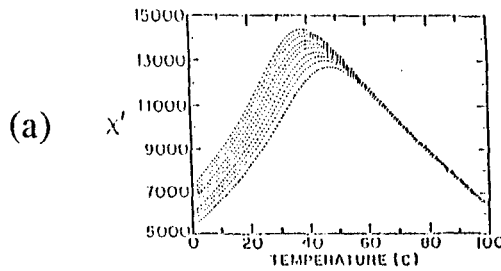


FIGURE 7 Projection of the Tungsten Bronze ferroelectric structure normal to the 4 fold c axis showing the sites for cation occupancy.

ELASTO-DIELECTRIC RESPONSE

Earlier studies have shown that the relaxor ferroelectric retain large values of RMS polarization to temperature some 100s of degrees above the dielectric maximum. In PMN, PLZT and SBN types measurement of lattice strain (thermal expansion) and optical refractive index^{12,13,14} show very good agreement in the prediction of the decay of RMS polization. The question as to whether the residual polarization is static or dynamic has been more difficult to decide. Measurement of electrostriction in SBN above T_m strongly suggested the dynamical model,¹⁵ but it is only very recently that careful neutron spectroscopy has completely confirmed the super-paraelectric behavior at higher temperature in PMN.

PMN-10PT AGE FREE

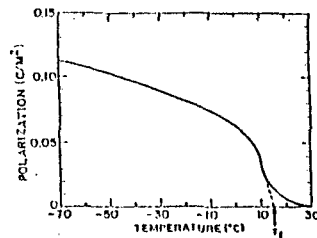
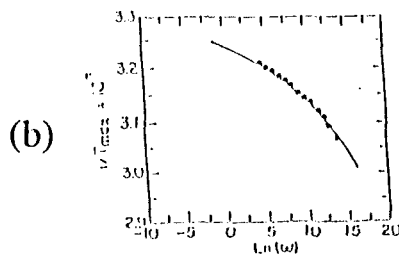


$$\omega = \frac{1}{\tau} = \frac{1}{\tau_0} \exp\left[\frac{-E_{fl}}{k(T - T_f)}\right]$$

activation energy of 0.0407 eV,

pre-exponential factor of 10^{12} Hz

freezing temperature of 291 K.



Vogel-Fulcher type freezing of polar fluctuations.

FIGURE 8 (a, b) Evidence for a glass like freezing of the dielectric response in PMN:PT solid solution lead in to Vogel:Fulcher type behavior with freezing temperature T_f .
 (c) Field cooled poled sample show “thawing” temperature T_f .

A key feature of the dielectric response is the strong dispersion in the weak field permittivity. Studies by Viehland et al¹⁶ have shown that the frequency/temperature characteristics are nicely described by the Vogel:Fulcher relation (figure 8a) and that the freezing temperature T_f deduced from this relation agrees closely with the thawing temperature where remanent polarization is lost on heating a field cooled sample (figure 8b). Vogel:Fulcher suggests a slowing down and freezing into a glass like ensemble of nano-domains, such a behavior would also suggest that the weakly cooperating nano-polar regions should begin to depart markedly from Debye like response towards a very long flat tail upon an ϵ^{11} corresponding to the freezing process and this is indeed observed (figure 9).¹⁷

For any precise dielectric studies it is essential to recognize and eliminate the aging process. As discussed earlier it is impossible to eliminate defects which couple to the polarization system in PLZT, since the La^{3+} doping necessitates that the sample have equivalent lead vacancies. In $\text{Pb}(\text{Mg}_{1/3}\text{Nb}_{2/3})\text{O}_3$ however the crystal is a compound, and if it is made with care from very high purity starting materials, macroscopic stoichiometry can be preserved in a fully stuffed structure. For this type of material aging can be eliminated (figure 10a), and the phenomenon can be reintroduced by a low level MnO doping. Figure 10b shows a MnO doped sample which has been aged at room temperature (20°C) then cooled to low temperature and reheated. Note the manner in which the relaxor response has been eliminated for all temperatures above the aging temperature, but is reintroduced at lower temperature. A full explanation is given in references 18 and 19 but is beyond the scope of this review. The data are emphasized however as it is clearly essential to ‘uncouple’ aging if time dependent properties of the relaxor are to be studied without gross perturbation.

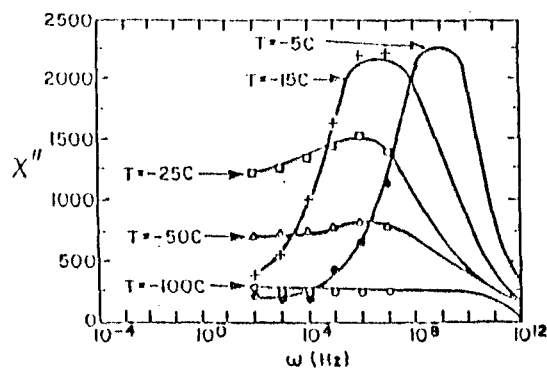


FIGURE 9 Glass like behavior of dielectric susceptibility χ^{11} .

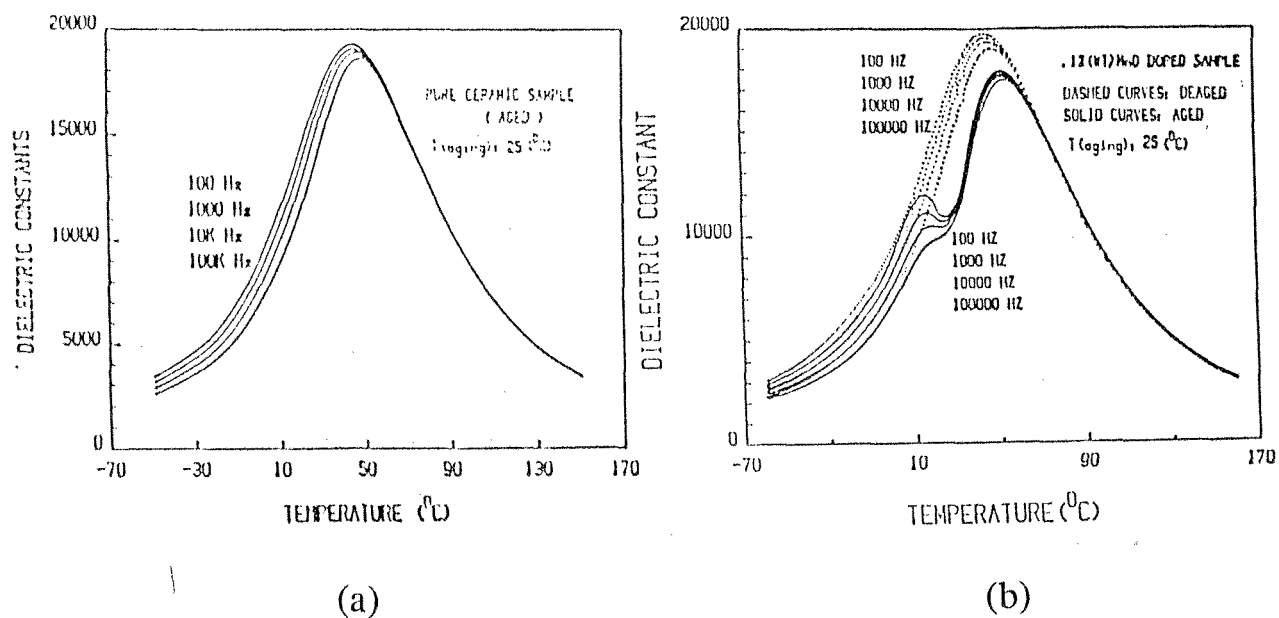


FIGURE 10 (a) “Clean” PMN:PT sample showing the absence of aging in ϵ^1 after 1,000 hours at room temperature.

(b) Aging behavior in PMN:PT reintroduced by low lever doping with MnO.

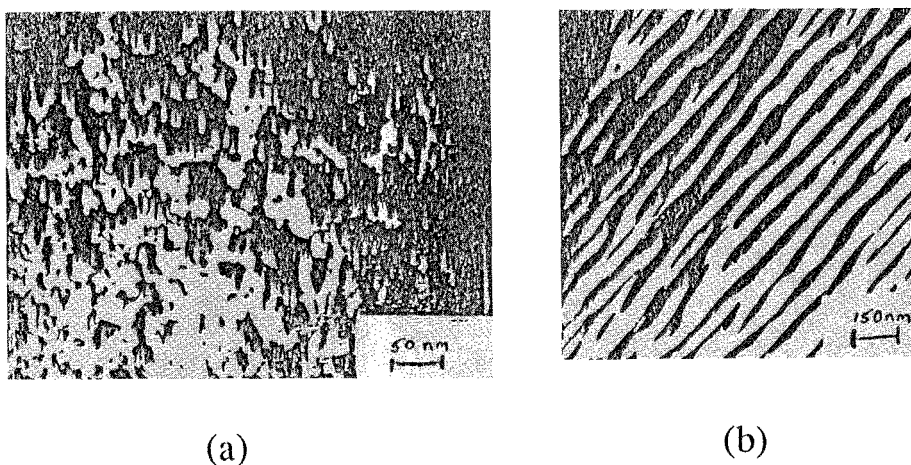


FIGURE 11 (a) Structure of nano-scale polar domains revealed in PLZT at the 8.2:65:35 composition by dark field TEM.

(b) Modification

To explore the high field response it is necessary to turn to the PLZTs and to take care to always study freshly de-aged samples. For an 8:2:70:30 PLZT composition Randall²⁰ has imaged using TEM the nano domain structure at low temperature (figure 11a) and by using charging from the beam current the evolution of nano-domains towards more normal continuous ferroelectric domains (figure 11b). Consequences of the application of static fields to PLZT samples which have been cooled in the zero field state have been explored by Yao Xi et al.²¹ Typical curves of switch over to a macro polar state on heating under bias are shown in figure 12a,b. If the system behaves as a spin glass the switch over should be modeled by the deAlmeida-Thouless relation²² and data taken from the measurements of Yao Xi et al are modeled in this manner in figures 13.²³

In deducing the RMS polarization it was tacitly assumed that the polarization related electrostriction constants Q_{11} , Q_{12} are independent of temperature in fact this has been proven by direct measurement (figure 14).²⁴ Clearly then in this circumstance one must expect that all the dielectric (Polarization) behavior will be reflected into the elastic response. The close relation between elastic and dielectric responses is evident in figure 15. For the high field response, it is to be expected that the high polarization values which can be induced anhyserically near T_m will give rise to large elastic strains. Values of x_{33} the strain in the field direction for a PMN:PT solid solution are shown in figure 16. The slope of this curve at any point is the effective d constant (d_{33}) which goes to very large values at relatively modest E fields.²⁵

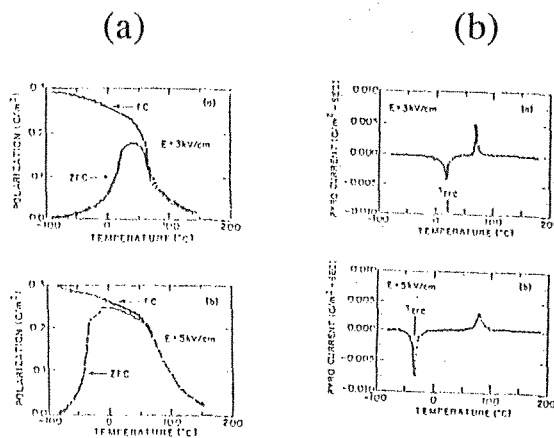


FIGURE 12 (a,b) Polarization and depolarization of PLZT 8:65:35 under field cooled and zero field cooled conditions as determined by integration of the pyroelectric response.

$$\dot{\epsilon} = \Lambda \left[\frac{T_f(0) - T_{zfc}(E)}{T_f(0)} \right]^{\frac{3}{2}}$$

deAlmeida-Thouless relationship

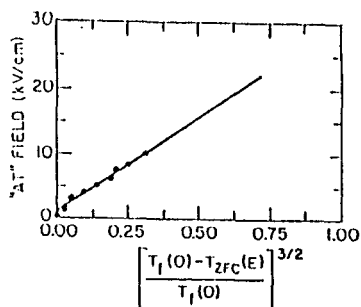


FIGURE 13 Data of 12(a) and similar studies at different field levels fitted to the deAlmeida-Thouless relation.

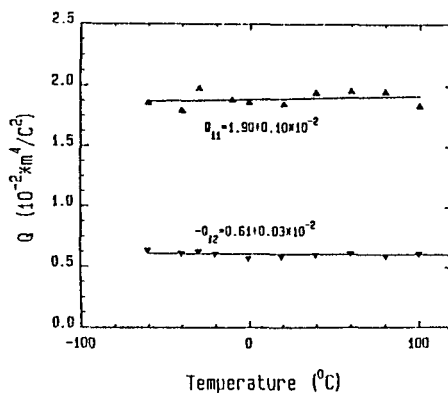


FIGURE 14 Ultradilatometer measurements of the electrostrictive constants Q_{11} , Q_{12} as a function of temperature in PMN:10 PT.

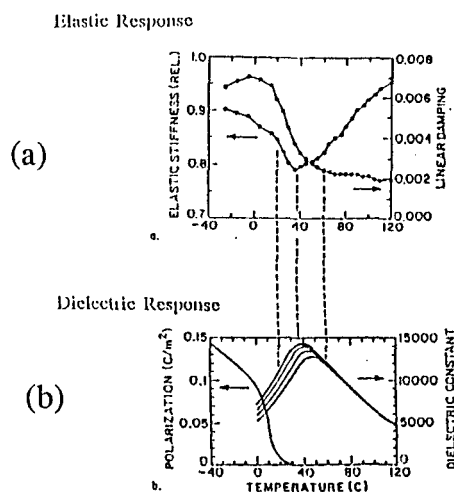


FIGURE 15 (a) Elastic stiffness and damping in ceramic PMN:10 PT.
(b) Comparison to dielectric softening associated with micro-polar behavior.

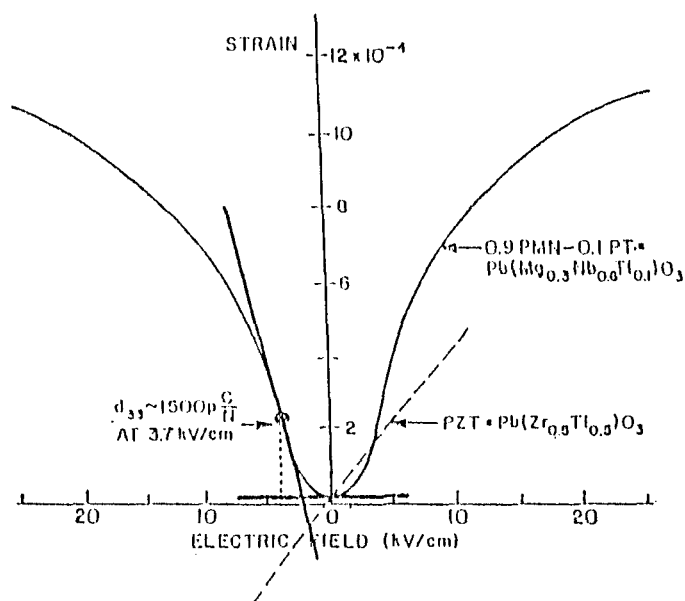


FIGURE 16 Strain vs. Field curve for PMN:10 PT illustrating the large values of induced piezoelectric d_{33} under DC field control.

TUNGSTEN BRONZE STRUCTURE RELAXOR FERROELECTRICS

In the solid solution system $\text{Sr Nb}_2\text{O}_6:\text{BaNb}_2\text{O}_6$ the end member compositions are not in the bronze structure, however in the range between $\text{Sr}_{0.8}\text{Ba}_{0.2}\text{Nb}_2\text{O}_6$ and $\text{Sr}_{0.3}\text{Ba}_{0.7}\text{Nb}_2\text{O}_6$ stable SBN bronzes form.²⁶ Across this range the prototypic structure is tetragonal and for fields in the 001 (c) axis direction the characteristics are these of a relaxor ferroelectric with polarization along (001). Both optical²⁷ and elastic²⁸ studies confirm that large values of RMS polarization persist to temperatures well above T_m and there is clear evidence of ferroelectric behavior at low temperature.²⁹ Dispersion near T_m becomes steadily more pronounced in compositions with increasing Strontium content.³⁰ For the congruently melting $\text{Sr}_{0.6}\text{Ba}_{0.4}\text{Nb}_2\text{O}_6$ excellent quality single crystals have been grown³¹ and the crystal is widely used in photorefractive applications.³²

The bronze system Lead barium niobate $\text{Pb}_{1-x}\text{Ba}_x\text{Nb}_2\text{O}_6$ (PBN) is of special interest as in the vicinity of the $\text{Pb}_{0.6}\text{Ba}_{0.4}\text{Nb}_2\text{O}_6$ composition there is a pseudo morphotropic phase boundary between orthorhombic and tetragonal ferroelectric forms (figure 17).³³ For the tetragonal form at the 57:43 composition the permittivity for fields along (001) shows a transition with only very weak dispersion and large thermal hysteresis (figure 18a), however for fields along (100) there is now a pronounced dispersion at lower temperature (figure 18b).

In compositions on the orthorhombic side of the MPB again the upper transition exhibited for fields along 100 is reasonably sharp, however, now there is a lower temperature relaxation for field in the 001 c axis direction. There are no evidences of phase transitions in either crystal in the

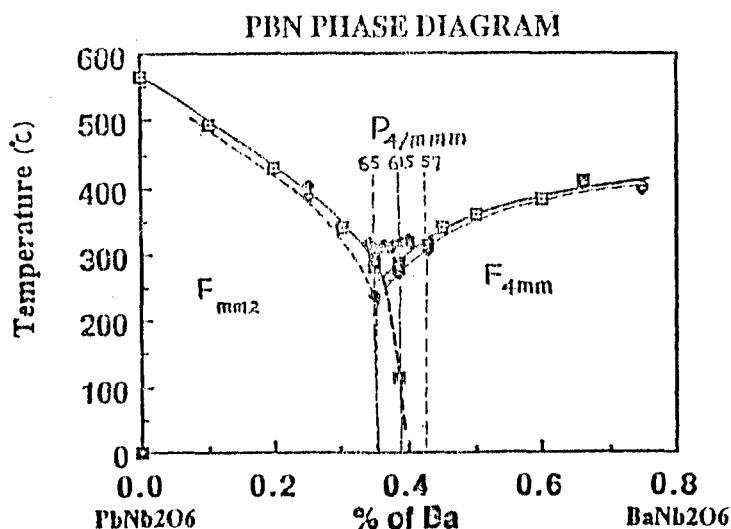
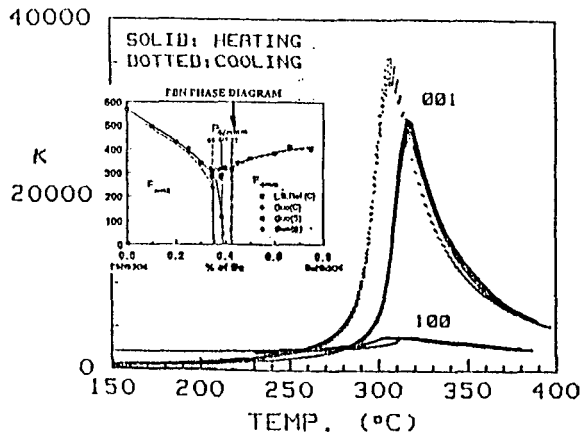


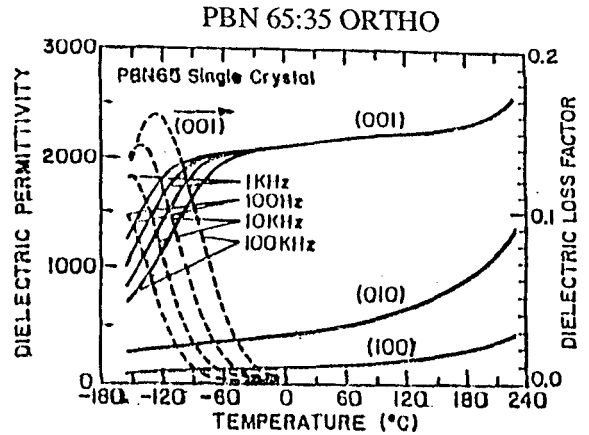
FIGURE 17 Phase diagram for the lead niobate:barium niobate system (PBN) showing the pseudo-morphotropic phase boundary near the 60:40 composition.

region of the dispersion, but cooling the crystal under a poling field orthogonal to the main polarization direction produces a clear remanence of order less than $1/20^{\text{th}}$ of the major polarization.³⁴ It is interesting to note that for compositions close to the MPB large orthogonal electric fields will switch the major component of P changing the symmetry from tetragonal to orthorhombic or vice versa. With symmetry change the lower frequency dispersion also changes axial direction always appearing normal to the major component of P .

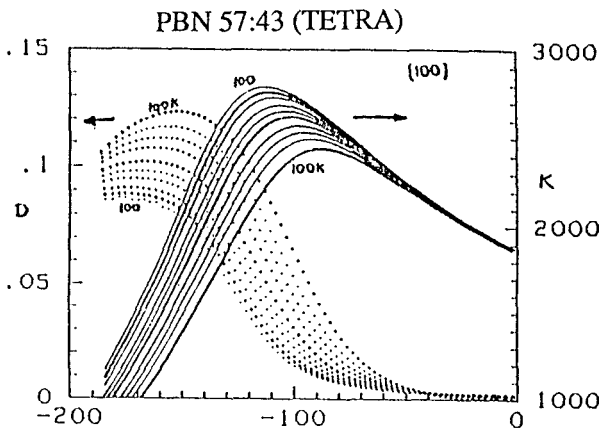
Clearly at low temperature, the field forced symmetry must be truly monoclinic in each case, as the P_s is tilted away from the primary axis (4 fold or 2 fold). Our suggestion is that in each case the micro polar regions which make up the mean polarization have P_s vectors which are slightly tilted away from the major axis. At the higher temperature transitions the energy barriers against polarization inversion are large and the dispersion weak, however the tilts perpendicular to P are random and dynamical, freezing out at the lower temperature dispersion. Crudely the energies envisaged are shown schematically for the "orthorhombic" and "tetragonal" macro symmetries in figure 19. The situation could be envisaged as that of a spin glass with two freezing temperatures for the orthogonal components of P . Magnetic systems which exhibit such phenomena have been studied.³⁵



(a)



(c)



(b)

FIGURE 18 (a) Dielectric response for fields along 001 and 100 directions for a composition in the tetragonal ferroelectric phase field (57:43) of PBN.

(b) Low temperature dispersive dielectric response for fields orthogonal to the major polar direction

(c) Dielectric response at low temperature in the orthorhombic phase for dields along 001.

Free Energy Model for Relaxor Ferroelectrics close to the MPB

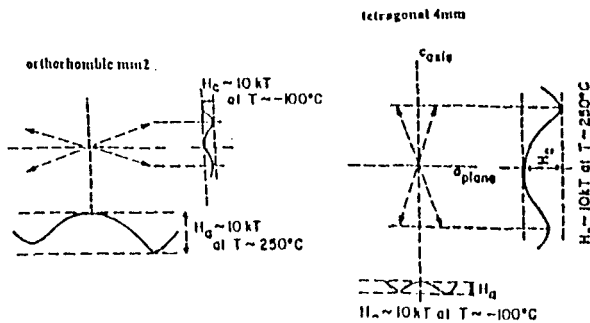


FIGURE 19 Proposed simple model for the anisotropic energetics of polar regions in the 'orthorhombic' and tetragonal relaxor phase fields of PBN.

THEORETICAL UNDERSTANDING

The relaxor ferroelectrics in the oxygen octahedron families are very complex solids so that it is certainly not surprising that in spite of some thirty years of continuous effort there is no comprehensive quantitative theory. It does appear that there is reasonably general agreement of the superparaelectric character at temperatures well above T_m but the detail of the kinetics of these regions and their mutual interaction as the temperature decreases is not clear.

An appealing simple model from A. Bell at EPFL³⁶ treats the micro region as a simple Devonshire ferroelectric, to calculate the activation energy ΔH as a function of size (assuming a simple spherical region). The distribution of activation energies then comes from a specific distribution of sizes, however to get good agreement with experiment (figure 20) it is still necessary to put in weak interaction between regions.

In a more general vein, Viehland et al have pointed up the many behavior features of the relaxors which suggest spin glass like features. Table II list many of these features, the small Y suggests a yes to the nature of the common feature in each case.

An alternative model which can again explain qualitatively most features of the relaxor appeals to random electric fields associated with the composition fluctuations as the origin of the break up of normal domain structure and the tremendous slowing down of the dynamics in PMN. For large non zero electric fields, it becomes difficult to explain the aging phenomena which occur in PLZT and in suitably doped PMN. For such crystals aging under a field as little as 3KV/cm is sufficient to wipe out the relaxation at room temperature and to lead to a poled ferroelectric structure on cooling under short circuit conditions. Evidently the kinetics is very sensitive to small fields generated by defect dipole systems. Perhaps a way out of this dilemma would be the suggestion that the random field is of elastic rather than electric origin.

Recent measurements of the poling of zero field cooled PMN does suggest³⁷ the presence of barkhausen pulses which could occur from the switching of ferroelectric micro-domains in concert with the random field model however it is not clear whether these measurements were carried out on aging free material.

In summary, many features of the chemo-elasto-dielectric behavior of relaxors are becoming more clear, even though there is not yet a comprehensive qualitative theory to explain the responses.

TABLE II Comparative list of physical properties of relaxors to spin and orientational glasses.

PROPERTY	RELAXOR	SPIN GLASS
Dispersion of Susceptibility	Y	Y
Dispersion of T_{max}	Y	Y
Freezing Temperature (T_f)	Y	Y
Imaginary Component Frequency Independent below T_f	Y	Y
Strong Nonlinear Response	Y	Y
Maximum Nonlinearities near T_f	Y	Y
Frustration	Y	Y
Susceptibility "Diffuse"	Y	Y
Deviations from Curie-Weiss Behavior	Y	Y
Analysis of Deviation for Local Order Parameter	Y	Y
Broadening of Relaxation Time Distribution on Cooling	Y	Y
Hysteresis, Irreversibility, and Remanence below T_f	Y	Y
Local polarization or magnetization	Y	Y
Local correlations between moments	Y	Y
Long range ordering in the Field Cooled State	Y	Y
Lack of anisotropy in the Zero Field Cooled State	Y	Y
De-Almedia Thouless Analysis	Y	Y
Polarization or Magnetization Viscosity	Y	Y
Chemical or Structural Inhomogeneity	Y	Y

PRACTICAL APPLICATION

One may judge the most likely areas of application for the relaxor ferroelectrics by considering the very unusual property combinations afforded in these systems. Table III outlines these properties. The very high dielectric permittivity is properly exploited in new multilayer ceramic capacitors. The very strong electrostrictive response does not depend on a domain contribution to the strain and is thus very largely reversible, a vital feature for precise actuators which cannot be servo controlled. The slope of the electrostrictive response as a function of field is the piezoelectric constant and d_{33} values much larger than those in conventional PZTs can be achieved under modest fields, giving a whole new family of potential agile transducers for sensing and actuation. Similarly under DC bias exceedingly large pyroelectric coefficients can be induced so for the bolometric long wavelength IR sensing and imaging the relaxors are of major interest.

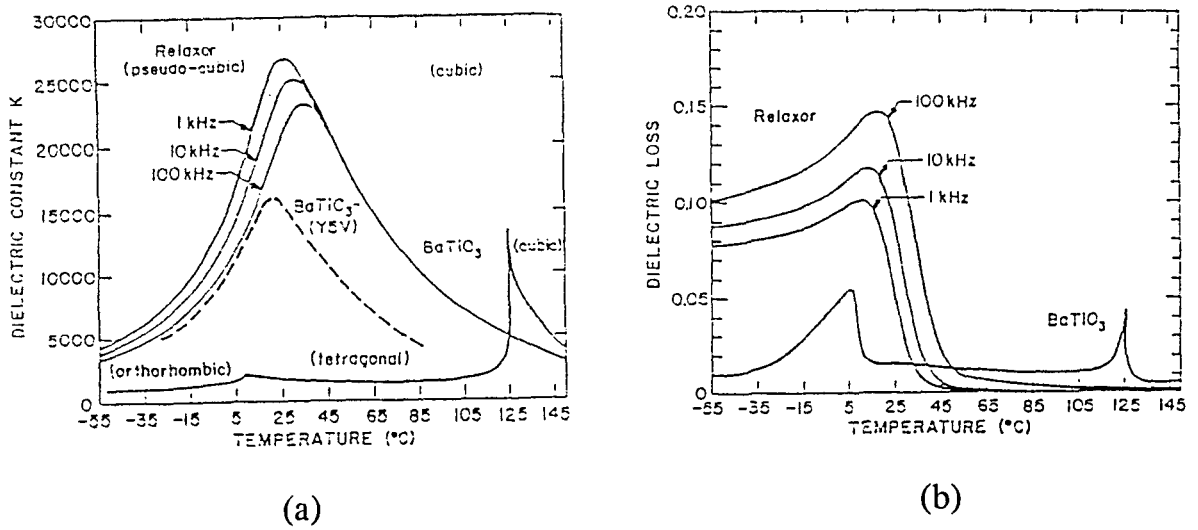
In the following brief description we confine attention to just the capacitor and actuator potential. For capacitor dielectrics, three features of the lead based relaxors are exceedingly attractive.

TABLE III Relaxor Properties which are of Interest for Practical Application.

PROPERTIES OF INTEREST

- HIGH DIELECTRIC PERMITTIVITY.
Multilayer Ceramic Capacitors.
Co-Fires with Copper Electrodes.
- VERY STRONG ELECTROSTRICTION.
Multilayer Electrostrictive Actuators.
Optical Telescope Adaptive Optics: Hubble Corrector.
- SWITCHABLE PIEZOELECTRIC RESPONSE.
Agile Transducers for Electromedical Applications.
- SWITCHABLE STRONG PYROELECTRICITY.
Long Wavelength Infra-red Pyroelectric Imaging Systems.

The dielectric permittivity for a typical PMN:10 PT relaxor (figure 20a) is significantly higher than equivalent Y5V type modified BaTiO₃ compositions. The loss level is also higher (figure 20b), but decays rapidly under bias field where MLC type capacitors are largely used. The bias behavior is also most attractive as the material retains high permittivity to higher fields than the



Relaxor: $(\text{PbMg}_{1/3}\text{Nb}_{2/3}\text{O}_3)_{0.9}(\text{PbTiO}_3)_{0.1}$

FIGURE 20 (a) Dielectric permittivity as function of temperature and frequency in relaxor $(\text{PbMg}_{1/3}\text{Nb}_{2/3}\text{O}_3)_{0.9}(\text{PbTiO}_3)_{0.1}$ compared with a modified BaTiO_3 Y5V commercial composition and with pure BaTiO_3 .
 (b) Dielectric loss in PMN:PT compared to the loss in pure BaTiO_3 .

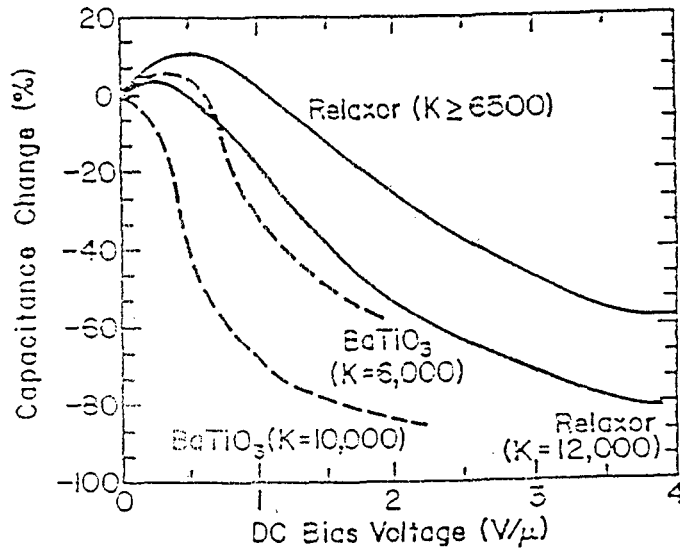


FIGURE 21 Dielectric saturation in the relaxor composition as compared to a BaTiO_3 based dielectric of similar permittivity.

conventional BaTiO_3 based materials (figure 21) and also the RC time constant is longer for the full range of working temperatures (figures 22). A further signal advantage for the tape case monolithic MLC structures is that the PMN type compositions can be co-fired with copper electrodes which is impossible with the BaTiO_3 based systems.

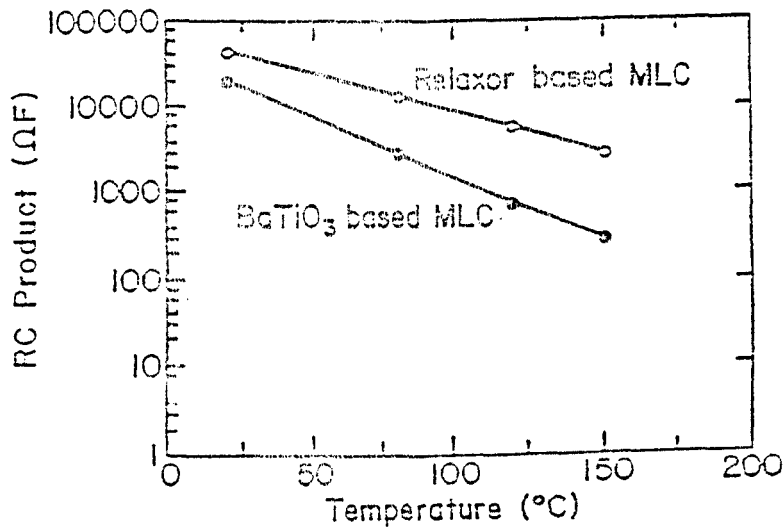


FIGURE 22 RC time constant as a function of temperature for the relaxor as compared to the BaTiO₃ based dielectric.

It is thus not surprising that the World's major capacitor companies are exploring a very wide range of these lead based relaxor compositions (Table IV).

In actuator application, the cardinal advantage of the PMN based relaxors is the very low hysteresis which can be obtained in the strain:voltage characteristic (figures 23a) in comparison to comparable soft PZT systems (figures 23b). A summary table for commercial actuator performance between PMN and PZT compositions is given in Table V. It is natural then to expect that electrostrictive relaxor actuators will be of most value where precise positioning is required and servo feedback control is not realizable. Such situations occur in a number of optical systems. One such system of very high visibility is a corrector for the troubled Hubble Space Telescope. This device is a tilt mirror (figure 24) which can be fully controlled from the ground by three PMN actuators. The function of a mirror is to permit precise alignment of a new optical train in the wide field camera which will contain elements configured to fully correct for the original improper figure of the primary mirror. The actuators are small multilayer PMN:PT stacks, figure 25 shows the dimension in comparison with the smallest American coin, the dime. The tilt mirror is just one of a range of optical components which begin to incorporate PMN active control and field in clearly ripe form any new products using these precise electro mechanical control elements.

TABLE IV
Composition families and associated companies involved in the application of relaxor type dielectrics to multilayer capacitors (Survey by the Penn State Dielectric Center).

Commonly Employed Perovskite End Members for Relaxor-Based					
Complex Perovskites	$+T_c(^{\circ}\text{C})$	++Behavior	Simple Perovskites	$T_c(^{\circ}\text{C})$	Behavior
[PMN]	-10	Relaxor-FE	PbTiO ₃	490	FE
[PZN]	140	Relaxor-FE	PbZrO ₃	230	AF
[PNN]	-120	Relaxor-Fe	BaTiO ₃	—	Para
[PFN]	110	Normal-FE	SrTiO ₃		
[PFW]	-95	Relaxor-FE			
[PMW]	38	AF			
[PNW]	17	AF			

+ Transition temperatures for relaxors are averages or at 1 kHz.

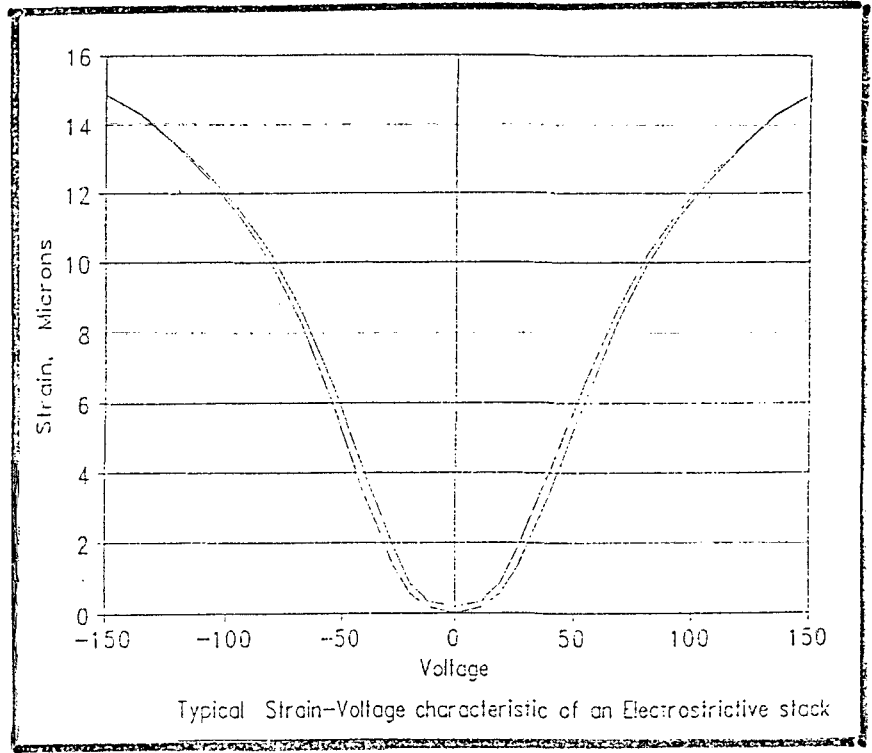
++ FE-Ferroelectric, AF-Antiferroelectric, Para-Paraelectric.

[PMN]:	Pb(Mg _{1/3} Nb _{2/3})O ₃	[PFW]:	Pb(Fe _{2/3} W _{1/3})O ₃
[PZN]:	Pb(Zn _{1/3} Nb _{2/3})O ₃	[PMW]:	Pb(Mg _{1/2} W _{1/2})O ₃
[PNN]:	Pb(Ni _{1/3} Nb _{2/3})O ₃	[PNW]:	Pb(Ni _{1/2} W _{1/2})O ₃
[PFN]:	Pb(Fe _{1/2} Nb _{1/2})O ₃		

Composition Families for Relaxor-Based MLCs

Composition	EIA Temp Specification	Manufacturer (Assignee)	Patents and Refs.
PLZT-Ag	X7R	Sprague	U.S. Pat. 4,027,209 (1973) Ref. 9
MPW-PT-ST	X7R	DuPont	U.S. Pat. 4,048,546 (1973)
PFN-PFW	Y5V	NEC	U.S. Pat. 4,078,938 (1978)
PFN-PFW-PZN	Y5V	NEC	U.S. Pat. 4,236,928 (1980)
PFN-PMT	---	TDK	U.S. Pat. 4,216,103 (1980)
PMN-PT	Y5V	TDK	U.S. Pat. 4,265,668 (1981)
PMN-PFN	Y5V	TDK	U.S. Pat. 4,216,102 (1980)
PMN-PFN-PMW	Y5V	TDK	U.S. Pat. 4,287,075 (1981)
PFW-PZ	Z5U	TDK	U.S. Pat. 4,235,635 (1980)
PFW-PT-MN	Z5U	Hitachi	U.S. Pat. 4,308,571 (1981)
PMN-PZN-PT	Z5U	Murata	U.S. Pat. 4,339,544 (1982)
PFN-PFW-PbGe (MSC)	X7R		Ref. 10
PFN-PFN-PNN	Z5U, Y5V	Ferro	U.S. Pat. 4,379,319 (1983)
PMW-PT-PNN	Z5U	NEC	U.S. Pat. 4,450,240 (1984) Ref. 11
PFN-BaCa(CuW)-PFW	Y5V	Toshiba	U.S. Pat. 4,544,644 (1985) Ref. 12
PMN-PZN	Z5U	STL	U.K. Pat. 2,127,187A (1984)
PMN-PFN-PT	Z5U	STL	U.K. Pat. 2,126,575 (1984)
PMN-PZN-PFN	Z5U	Matsushita	Japan Pat. 59-107959 (1984)
PMN-PFW-PT	---	Matsushita	Japan Pat. 59-203759 (1984)
PNN-PFN-PFW	Y5V	Matsushita	Japan Pat. 59-111201 (1984)
PZN-PT-ST	---	Toshiba	Ref. 13
PMN-PFN-PbGe	Z5U	Union Carbide	U.S. Pat. 4,550,088 (1985)
PFN-PNN	Y5V		Ref. 14
PFW-PFN (MSC)		NTT	Refs. 15-17
PMN-PT-PNW	Z5U	Matsushita	Ref. 18
PMW-PT-PZ	X7R	NEC	Ref. 19
PZN-PMN-PT-BT_ST	Z5U	Toshiba	Japan Pat. 61-155245 (1986)
PZN-PT-BT-ST	X7R	Toshiba	Japan Pat. 61-250904 (1986)
PZN-PMN-BT	Y5U, Y5S	Toshiba	Ref. 20
PMN-PLZT	Z5U	MMC	U.S. Pat. 4,716,134 (1987)
PMN-CT, ST, BT	Z5U	Matsushita	Japan Pat. 62-115817 (1986)
PFW-PFN-PT	Y5V		Ref. 21
PT-PMN-PZN (MSC)	X7R, X7S	Toshiba	U.S. Pat. 4,767, 732 (1988)
PMN-PS-PNW-Ca (Base Metal)	Z5U	Matsushita	Refs. 22-23

(a)



(b)

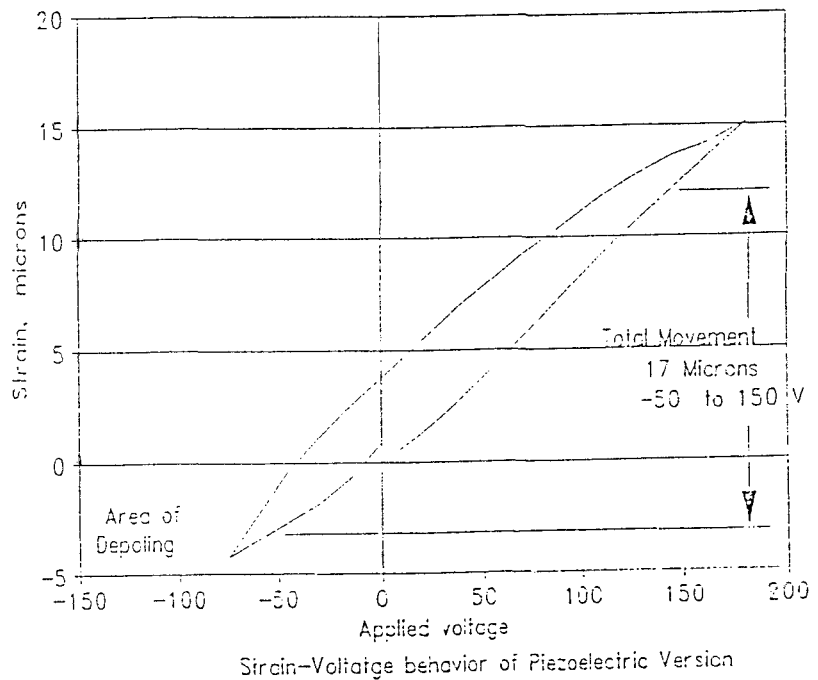


FIGURE 23 (a) Anhyseritic nonlinear strain (x_3) versus field cure for PMN:PT relaxor multilayer actuator.
 (b) Strongly hysteritic response of a comparable multilayer soft PZT piezoelectric actuator.

TABLE V Comparison of the salient features of the relaxor based actuator as compared to the more conventional soft PLZT system.

Comparative Parameters of Piezoelectric vs Electrostrictive Stacks
(Both 20mm long, 6mm diam, 150 V Rated)

Parameter	Condition	Electro	Piezo	Units
Capacitance	25°C	4	1	μ-F
Diss. Factor	25°C	8	3	%
Frequency	Lose <10% strain	100	1000	Hz
Force	Lose <10% strain	700	450	Newtons
Extension	at 150 VDC	16.5	15	Microns
Hysteresis	25°C	<2	>15	%
Creep	After 24 hours	<2	≈5	%
Temp Range	Keep 75% strain	±20	0-100	°C
TCE	25 - 125°C	<1	1.6	ppm/°C
Youngs Modulus	25°C	16	4	10 ⁶ PSI
Response Time	25°C	<100	<5	μ-sec

JPL WF/PC-2 ARTICULATING FOLD MIRROR (AFM)

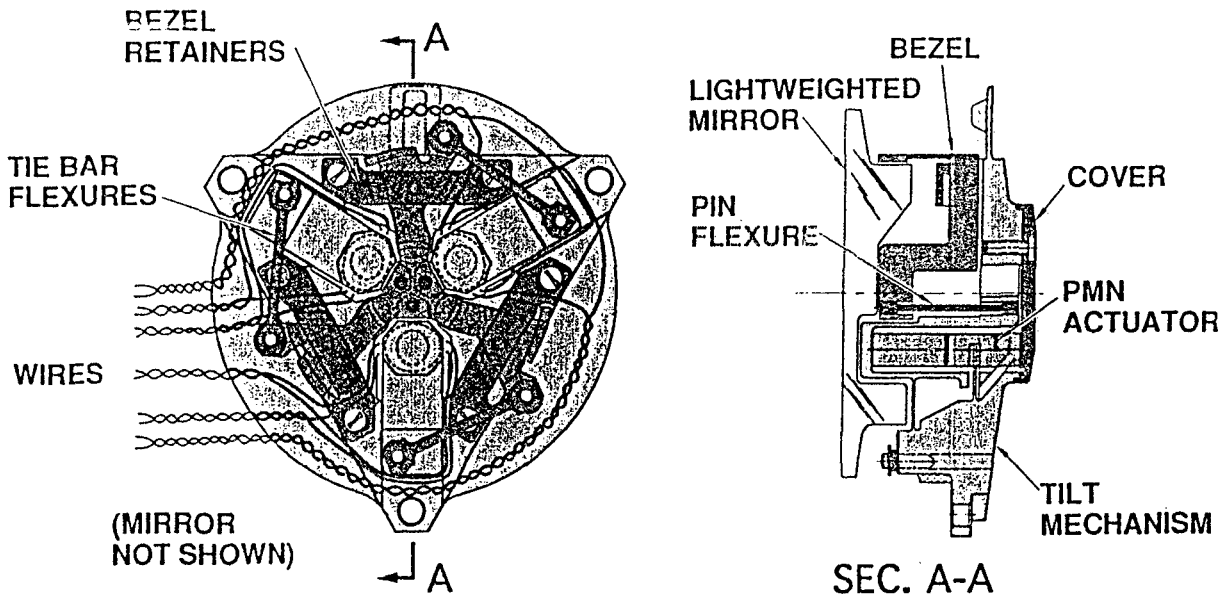


FIGURE 24 Plan and elevation views of the JPL Articulated fold mirror driven by PMN:PT actuators (Corrector to be flown December 1993).

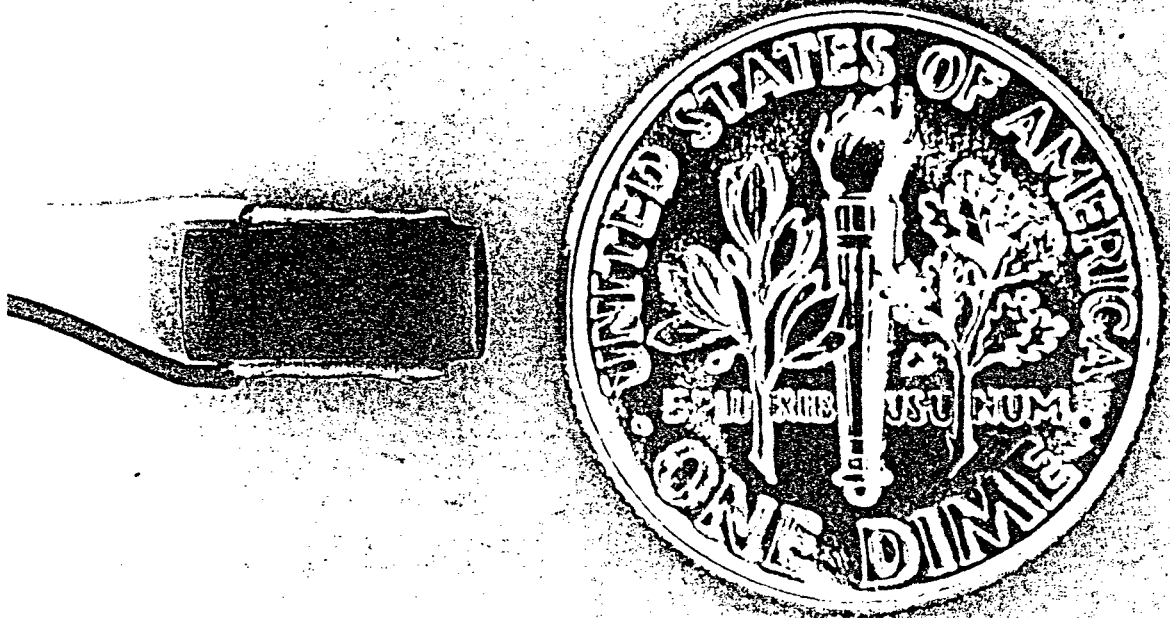


FIGURE 25 Scale of the multilayer PMN:PT actuator as compared to an American dime coil.

REFERENCES

1. G. S. Smolensky, A. Agronovskaya, Soviet Physics Solid State **1**, 1429 (1960).
2. V. Bokov and I. Mylnikova, Soviet Physics Solid State **3**, 3 (1960).
3. C. Randall and A. Bhalla, J. Mat. Sci. **29**, 5 (1990).
4. J. Chen and M. Harmer, J. Am. Ceram. Soc. **72**, 593 (1989).
5. C. Randall, PhD Thesis, University of Essex, Colchester, England (1987).
6. A. Katchaturyan, Private Communication.
7. N. Setter, PhD Thesis, Pennsylvania State University (1980).
8. C. Randall, D. J. Barber, and R. W. Whatmore, Journal of Microscopy **145** (3), 275 (1987).
9. G. Rossetti, PhD Thesis, Pennsylvania State University (1993).
10. W. A. Schulze, J. V. Biggers, and L. E. Cross, J. Am. Ceram. Soc. **61**, 749 (1980).
11. M. P. Leffler, MS Thesis, Pennsylvania State University (1989).
12. G. Burns and F. Dracol, Solid State Commun. **48**, 853 (1983).
13. P. Asadipour, U. Kumar, S. J. Jang, A. S. Bhalla, and L. E. Cross, Jpn. J. Appl. Phys. **24** (2), 742 (1985).
14. A. S. Bhalla, R. Guo, L. E. Cross, and G. Burns, Phys. Rev. B. **36** (4), 2030 (1987).
15. P. Asadipour, MS Thesis, Pennsylvania State University (1986).
16. D. Viehland, S. J. Jang, L. E. Cross, and M. Wuttig, J. Appl. Phys. **66**, 2916 (1990).
17. D. Viehland, M. Wuttig, and L. E. Cross, Ferroelectrics **120**, 71 (1991).
18. W. Pan, E. Furman, G. O. Dayton, and L. E. Cross, J. Mat. Sci. Letters **5**, 647 (1986).
19. W. Pan, Q. Zhang, and L. E. Cross, J. Am. Ceram. Soc. **71**, C17 (1988).
20. C. Randall, D. Barbes, and P. Groves, J. Mat. Sci. **21**, 4456 (1986).
21. Y. Xi, C. Zhilli, and L. E. Cross, J. Appl. Phys. **54**, 3399 (1983).
22. J. deAlmedia and D. Thouless, J. Phys A **11**, 983 (1978).
23. R. Chamberlin, M. Hardiman, L. Turkevich, and R. Orbach, Phys. Rev. B **25**, 6720 (1982).
24. W. Pan and L. E. Cross, ONR Annual Report for 1985 on contract N00014-82-KO339 (July 1986).

25. W. Pay, W. Y. Gu, D. J. Taylor, and L. E. Cross, Jpn. J. Appl. Phys. **28** (4), 653 (1989).
26. A. M. Glass, J. Appl. Phys. **40**, 4699 (1981).
27. G. Burns and F. H. Dacol, Ferroelectrics **104**, 25 (1990).
28. G. Burns, Phase Transitions **5**, 261 (1985).
29. T. Cline, PhD Thesis, Pennsylvania State University (1979).
30. M. E. Lines and A. M. Glass, Principles and Applications of Ferroelectrics and related materials, Clarendon, Oxford (1977).
31. R. R. Neurgaonkar and W. K. Kory, J. Opt. Soc. Am. **3(B)**, 274 (1986).
32. E. J. Sharp, W. W. Clark III, M. Miller, G. L. Wood, B. Monson, and G. J. Salamo, Applied Optics **29** (6), 743 (1990).
33. M. H. Francombe, Acta. Cryst. **13**, 131 (1960).
34. R. Guo, A. S. Bhalla, C. Randall, and L. E. Cross, J. Appl. Phys. **67** (10), 6405 (1990).
35. A. Schröder, J. Fisher, H. von Lohneysen, W. Bauhofer, and U. Steigenberger, J. Phys (Paris) Colloq (to be published).
36. A. Bell, J. of Physics: Condensed Matter (submitted).
37. V. Westphal, W. Kleemann, and M. D. Glinchuk, Phys. Rev. Letters (**68** (6), 847 (1992)).

L. Eric Cross is an Evan Pugh Professor of Electrical Engineering at the Materials Research Laboratory of The Pennsylvania State University. Professor Cross took his BSc (Honors Physics) at Leeds University in 1948, and completed his PhD in Physics in 1953. He was a University Scholar, an Assistant Professor and an ICI fellow in the Department at Leeds. After a short period at the Electrical Research Association in Leatherhead Surrey, he moved to the USA to take up a position in the developing Materials Research Laboratory (MRL) at Penn State. He was the Laboratory Director from 1985 to 1989.

Dr. Cross is a member of the National Academy of Engineering, Fellow of the American Institute of Physics, of the American Ceramic Society, the IEEE, and the American Optical Society and a member of the Japanese Physical Society. He is chairman of the IEEE committee on ferroelectrics, US representative for ferroelectrics on IUPAP, and a member of the Defense Sciences Research Council of DARPA. His interests are in dielectric and ferroelectric crystals, piezoelectric and electrostrictive ceramics and composites for sensor, actuator and transducer applications, and as components in "smart" materials and structures. He has co-authored more than 300 technical papers and sections of six books.

